govských a difuzních maxim a který dokládá uťitečnost a názornost uvedeného přístupu.

# A NEW APPROACH TO TREATMENT OF POWDER DIFFRACTION DATA

## Lubomír Smrčok

*Institute of Inorganic Chemistry SAS, SK-812 36 Bratislava, Slovak Republic*
*e-mail : uachsmrk@savba.sk*

The discrete wavelet transform (DWT) and the level-dependent soft-thresholding method (MAD) can be applied to any experimental data set in order to remove the statistical noise. Wavelets are a family of basis functions that can be used to approximate measured signals either in one or in multiple dimensions.

In this talk, examples of wavelet denoising of powder diffraction patterns will be given. It was found that wavelet denoising in contrast to polynomial filters neither shifted nor distorted the diffraction profiles.

Another use of the above mentioned technique is its application to the Rietveld refinement on powder data (structure determination with atomic resolution). Crystal structures of triclinic kaolinite, cubic HMT and a part of the structure of a monoclinic rare sugar were refined using wavelet compressed sets of intensities. It was found that accuracy of refined positional parameters did not significantly change. Similarly, quantitative phase analysis of a three-component mixture done by Rietveld method provided very close estimates of phase composition. Moreover, application of DWT compressed data reduced the time needed for the refinement by 50-60 %.

# DETERMINATION OF CRYSTAL STRUCTURES OF SUGARS BY POTENTIAL ENERGY MINIMIZATION METHOD

## M. Ďurík

*Institute of Inorganic Chemistry, Slovak Academy of Sciences, Dúbravská cesta 9, 842 36 Bratislava, Slovak Republic*

Crystal structures of two rare sugars (RKSA1 - monoclinic, $P2_1$ and RKSA5 - hexagonal, $P6_2$, both $C_{13}H_{20}N_2O_5$) were predicted by potential energy minimization method. Molecular models were build on the basis of the positions of all atoms (40 atoms per molecule included hydrogens) derived from already known crystal structures [1,2]. Molecules were supposed to be rigid and no hydrogen bonds were taken into account. Two types of atomic charges were used: Mulliken (M) and those based on the fits to the molecular electrostatic potential (E). Potential energy was approximated as sum of three terms: electrostatic, attraction and repulsion. The second and the third terms were evaluated using empirical force fields. Two types of the force fields were applied: Dreiding (D) [3] and Williams (W) [4]. Positions of rigid molecules within unit cell were sought in eight simulation runs with twenty trial crystal structures per run. Simulations were done with the cell parameters set to the values obtained from the crystal structure (not optimized) and with the cell parameters optimized. Potential energy was minimized by global minimization method - simulated annealing implemented in the program Hardpack [5].

Subsequently, each generated powder pattern was compared by means of Rietveld refinement [6] to experimental powder diffraction pattern collected on a STOE Stadi P diffractometer. Refined parameters were only a scale factor, overall temperature parameter, W profile parameter and zero-point. In some cycles also lattice parameters were included.

Correct crystal structures of both sugars were found in the simulations done without optimization of the cell parameters, except for the M/D combination for RKSA1 and E/D for RKSA5. Prediction with optimization of cell parameters for RKSA1 was successful in all four combinations of atomic charge types and force fields. On the other hand in the case of RKSA5, calculations with optimized cell parameters did not provide acceptable crystal structures.

[1] Steiner, B., Koóš, M., Langer, V., Gyepesová, D., Smrčok, Ľ : *Carbohydr. Res.,* **311**, (1998), p. 1-9.

[2] Langer, V., Gyepesová, D., Smrčok, Ľ., Steiner, B., Koóš, M. : *Acta Cryst.* (1999) Submitted.

[3] Cox, S., Hsu, L.-Y., Williams, D.E. : *Acta Cryst.*, A**37**, (1981), p. 293 - 301.

[4] Mayo, S.L., Olafson, B.D., Goddard III, W.A., : *J. Phys. Chem.*, **94**, (1990), p. 8897-8909

[5] Rudert, R. : Hardpack, *Acta Cryst.*, A**52**, (1996), C-94.

[6] Rodriguez-Carvajal, J. : FullProf 3.5, LLB (1998) Private communication.

# CRYSTAL STRUCTURES OF LANTHANIDE COMPLEXES WITH TETRAAZAMACROCYCLIC LIGANDS

## P. Vojtíšek

*Universita Karlova, Department of Inorganic Chemistry, Albertov 2030, 128 40 Prague 2, Czech Republic*
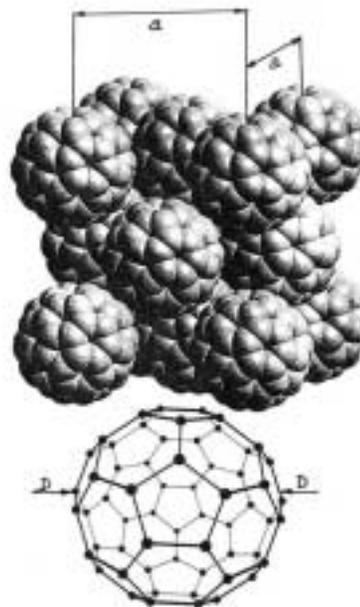
Complexation chemistry of yttrium and lanthanides is widely investigated because of the importance of medicinal use, e.g., gadolinium complexes as contrast agents in magnetic resonance imaging, yttrium-90 complexes in radio-immunotherapy, and luminiscent europium and terbium complexes as probes. To produce complexes with utilisation, it requires chelates with enhanced stability and kinetic inertness. A number of aminopolycarboxylic acids both acyclic and macrocyclic was tested . The first contrast agent that was aplied in humans was $[Gd(DTPA)(H_2O)]^{2-}$ [1], soon followed by $[Gd(DOTA)(H_2O)]^-$ [2]. In addtion, many derivatives of ligands were designed, synthesised and studied to improve properties of contrast agents which could both remain in the body longer and be targed toward specific tissues.

Some years ago, a study of derivatives of DOTA with side chains containing a methylenephosphonic ($-CH_2PO_3H_2$) or methylphosphinic ($-CH_2P(R)O_3H$) groups was begun [3], in a search for ligands with different properties than carboxylic compounds.
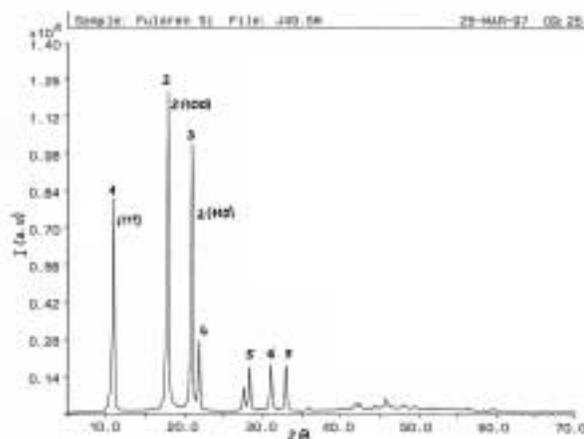
The phosphinic acids derivatived from cyclen (1,4,7,10-tetraazacyclodecane) are ligands similar to DOTA, but the presence of the tetrahedral phosphinic group gives (in contrast with corresponding carboxylic derivatives) an additional possibility for R,S-isomerism. The lanthanide complexes of tetrakis(phenylphosphinic) acid show R,S,R,S-configuration on the phosphorus atoms in crystals, in contrast to the previous published tetrakis-(benzylphosphinic) derivatives [3].

The similar, but unsymmetric, methyl-tris (phenyl-phosphonic) acid forms the electroneutral dimeric lanthanide complexes. These compunds show interesting structures based on the centrosymmetrical eightmembered ring which is typical for phosphinates, and further they contain eight- or nine coordinated Ln-unites with tetragonal antiprismatic or capped tetragonal antiprismatic arragement. This type of coordination is same for all phosphinic ligands and typical for „ DOTA-family" lanthanide complexes mentioned above. The serie of seven probably isostructural compounds with methyl-tris (phenylphosphinic) ligand enables to observe the effects of $Ln^{3+}$ radii on the geometry of coordination polyhedrons.

[1]   S. Aime, P. Ascenti, B. Comoglio, M. Fasano, S. Paoletti, *J. Am. Chem. Soc.*, **117** (1995) 9365,  S. Aime, M. Botta, G. Ermondi, *Inorg. Chem.*, **31** (1992) 4291.

[2]   M.F. Loncin, J.F. Desreux  & E. Mercing, *Inorg. Chem.,* **25** (1986) 2646.

[3]   D. Parker, *Chem. Soc. Rev.,* **1990** , 271,  S. Aime, A.S. Batsanov, M. Botta, R.S. Dickins, S. Faulkner, C.E. Foster, A. Harrison, J.A.K. Howard, J.M. Moloney, T.J. Norman, D. Parker, L. Royle  & J.A.G. Williams, *J. Chem. Soc., Dalton Trans.,* **1997**, 3623.

---

**Structure and some properties of fullerites**

# STRUKTURA A NĚKTERÉ VLASTNOSTI FULERITU

## Lubomír Sodomka[1], Jaromír  Sodomka[2], Bohuslav Knob, Vítek Šprta[3]

[1]*Technická univerzita v Liberci, Horská 16, 46014 Liberec 14,CR*

[2]*ČVUT Praha Fakulta dopravní Konviktská 20 Praha 1*

[3]*VUANCH Ústí nad Labem Revoluční 86*

### 1.  Úvod

Fulerity jsou krystalová nadstavba fulerenů, uhlíkových uzavřených molekul, z  nichž nejrozšířenější je fuleren C60 se šedesáti uhlíky v rozích komolého dvacetistěnu (s-ikosahedru) (obr.1). Tato molekula poprvé popsána v roce 1985 [1],  jejíž spolubjevitelé byli poctěni v roce 1996 Nobelovou cenou za chemii [2] , prohlášená také molekulou roku v roce 1991, se stala v současnosti předmětem zájmu výzkumu. Dnes už existuje  o fulere-



Obr. 1 (nahoře), Obr. 2 (dole)



Obr. 3

nech, fuleritech a fuleridech velké možství publikací od původních prací , přes souborné práce dokonce v češtině [3, 4, 5, 6]  k populárně vědeckým [7, 8] až k monografiím [9, 10] a sborníkům z konferencí [11].

Fulerit je nadmolekulární struktura molekul fulerenu C60. V něm kulové molekuly C60 vytvářejí vrstvením typu ...ABCABC... nadmolekulární plošně středěnou krychlovou strukturu zobrazenou na obr.2. Tato struktura byla prozatím jako jediná z vrstvových struktur pozorována a je zajimavé, že další jednoduchá struktura s těsným směstnáním jako je vrstvení ... ABABAB... dávající hexagonální mřížku s těsným směstnáním nebyla dosud objevena.

### 2.  Rentgenospektrální analýza fuleritu

Pro studium struktury byl vybrán fulerit dodávaný firmou Hoechst, Německo. Dodané vzorky obsahovaly
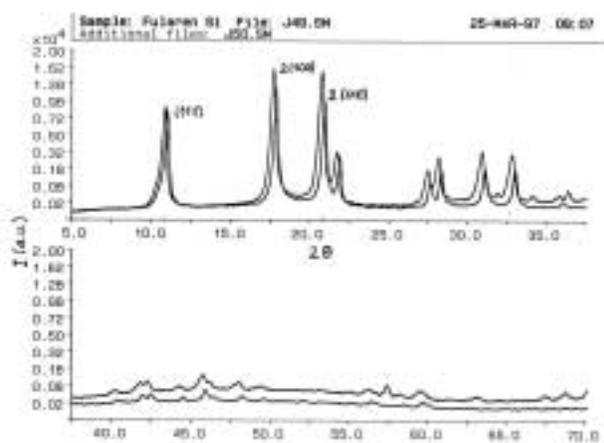
Obr. 4

99,78 w% uhlíku. Takťe 0,22 w% připadalo na ostatní prvky. K identifikaci a ke kvantitativní analýze 0,22w% příměsí byla provedena rentgenová spektrální analýza. Vzorky fulertu byly rozdrceny na jemný prášek, který byl nanesen na monokrystaly křemíku o průměru 30mm a vloťeny do rentgenospektrální aparatury firmy Philips PW1404 s rhodiovou anodou pracující při napětí 80kV s monochromátory z lithiumfluoridových krystalů s reflexí na rovinách (220) a s germaniovými krystaly pracujícími na rovinách (111). Z měření bylo zjištěno takovéto zastoupení příměsových prvků: síra 0,1063w%, barium 0,0801w%, argon 0,0275w%, osmium 0,0020w%, ťelezo 0,0016w%, zinek 0,0015w%. Zbytek tvoří lehké prvky do prvku 10, které se nedají rentgenovou spektrální analýzou snadno zjistit. Poloha jednotlivých prvků v mříťce fulertu nebyla uťitou metodou zjistitelná. Příměsi se mohou nacházet uvnitř fulerenových molekul, nebo mohou být interkalovány uvnitř fuleritové mříťky (viz obr.2).

## 3. Rentgenová difrakční analýza fulertu

K určování krystalové struktury vzorků fulertu byla provedena rentgenová strukturní analýza. K ní byl užit difraktometr Philips s měděnou rentgenkou s monochromátorem a Sollerovými clonami pracující na vlnové délce rentgenového záření 0,154nm (CuKα). Na vzorcích byly pořízeny difraktogramy v úhlovém intervalu dvojnásobného Braggova úhlu od 5 do 70 až 80 stupňů. Difraktogramy fulertu jsou na obr.3. Na obr 4. jsou společné difraktogramy původního krystalického vzorku před a po mletí. Z něho je vidět, že difrakční křivky mletého fulertu jsou posunuty směrem k menším Braggovým úhlům tedy k větším mezirovinovým vzdálenostem.

Z difraktogramů na obr.3 a obr.4 po oindexování difrakčních čar užitím 12 byly určeny Braggovy úhly difrakčních čar a z nich pak mezirovinové vzdálenosti., mřížkové parametry a průměr koulí fulerenu C60 Z rentgenových difrakčních záznamů byla ověřena pro měřený fulerit krychlová plosně středěná mřížka, jak je zobrazena na obr.2. V mřížkových bodech leží molekuly fulerenu C60 (obr.1). Z jednotlivých rentgenodifrakčních reflexí očíslovaných v pořadí od malých Braggových úhlů 1,2,3,4,5,6,7,8,9 postupně na rovinách (111),2(100),2(110)

a dalších byly určeny mřížkové parametry a1 = 1,64 nm, a2 = 1,1 nm, a3 = 1,316 nm, a5 = 1,16 nm, a6 = 1,07 nm, a7 = 1,07 nm, a8 = 1,12 nm, a9 = 1,22 nm.Z a3 byl určen průměr fulerenové koule D = 0,66 nm. Z teoretických výpočtů v [10] na str.63 byl určen průměr fulerenové koule D = 0,71 nm. Nižší naměřenou hodnotu lze vyložit vzájemným přitahováním fulerenu ve fulertu a stlačením pružné fulerenové koule. Různé hodnoty mřížkových parametrů fulertu z reflexí na různých krystalových rovinách lze vyložit stlačováním pružných fulerenových koulí v různých směrech a jejich geometrickou anizotropií.

## 4. Některé vlastnosti fuleritů

V odkaze [10] jsou uvedeny nejrůznější vlastnosti fuleritů jako je elektrická vodivost, fotovodivost a luminiscence. Tyto vlastnosti byly hledány rovněž i na zkoumaných vzorcích fulertu. Měření měrného odporu ukázala hodnotou větší než $10^{14}\Omega.m$, že je téměř nevodivý. Fotovodivost indukovaná dusíkovým laserem a kryptonovou výbojkou měla stejnou hodnotu jako vodivost elektrická. Z luminiscencí byla zjišťována fotoluminiscence buzená stejně jako fotovodivost dusíkovým laserem a kryptonovou výbojkou a nebyla u sledovaného vzorku fulertu pozorována stejně jako mechanoluminiscence [13]. Vzhledem k tomu, že uvedené měřené vlastnosti jsou strukturně citlivé a v citovaných pracech nebylo uvedeno složení a množství příměsí ve fuleritech, nejsou rozdílné výsledky měření překvapující.

## 5. Zhodnocení a závěr

Řešení struktury fulertu ukázala, že fulerit tvoří krychlovou plosně středěnou mřížku s mřížkovými body molekul kulového fulerenu C60. Vlivem přitažlivých vazebných sil a elasticitě molekul fulerénu C60 je mřížka v určitých směrech s menší hustotou molekul C60 deformována a tak průměr kulové molekuly fulerenu ve fulertu má nižší hodnotu 0,66 nm než byl teoreticky určený průměr izolované molekuly C60, který byl stanoven na hodnotu 0,71 nm. Rentgenospektrální analýza ukázala na přítomnost příměsí, a to nejvíce síry 0,1063w% a baria 0,0810 w%. Tyto a další příměsi neovlivnily elektronové vlastnosti zkoumaného fulertu, aby poskytly měřitelnou elektrickou vodivost, fotovodivost a luminiscenci fulertu.

*Příspěvek je věnován památce na nedožité 20. narozeniny Magdaleny Sodomkové.*

## Literatura

1. Kroto, H.V., et al.: *Nature* **318** (1985)162.

2. Sodomka,L.: Nobelova cena za objev fulerenu. MFI 7 (1997) 63; Sodomka,L., Sodomková, M.: Nobelovy ceny za fyziku. SetOut Praha 1997.

3. Matyáš,M.: Fullereny a fullerity. *PMFA* **37**(1992)288

4. Jech,Č.: Fullerenová allotropní forma uhlíku. *Čs.čas.fyz.* **42**(1992) 337.

5. Kraetschmer, W.: *AvH-Magazin* No.62, Dezember 1993, str.11.

6. Sodomka, L.,Sodomka, J.: Historie objevu fulerenů a jejich derivátů. *MFI* **8**(1998)216.

7. Sodomka, L., Sodomka, J.: Diamanty a ježci v kleci *T97* **40**(1997)22.

8. Valenta, J.: Nejkulatější molekula. *Vesmír* **76**(1997)65.

9. Koruga,G., et al.: Fullerene C60. North Holland, Amsterodam 1993.

10. Dresselhaus,M.S., et al.: Science of fullerenes and carbon nanotubes. Academic Press New York 1996.

11. Andreoni,W.: The chemical physics of fullerenes 19 (and 5) years later..NATO ASI Series, E:Applied Science vom 316 Kluwer Academic Publisher, Dordrecht 1996.

12. Sodomka, L.: Rentgenová difraktografie pevných látek, SNTL Praha 1960, str.116-136.

13. Sodomka,L.: Mechanoluminiscence a její použití. Academia Praha 1985.

# CRYSTAL STRUCTURE PARAMETERS AS A MEASURE OF THE DEGREE OF SHOCK METAMORPHISM IN QUARTZ

## Roman Skála

*Czech Geological Survey, Klárov 3/131, CZ-11821 Praha 1, Czech Republic, author's e-mail address:*
*skala@cgu.cz*

**Introduction:** Quartz is ubiquitous mineral phase in Earth crustal rocks. This is the reason why specific shock-wave generated features in quartz are used as indicators of high dynamic pressures due to hypervelocity impacts. Various techniques have been employed to study the shock effects in naturally shocked quartz (for details see e.g. [1-6] and references therein). The literature on shock metamorphism of quartz contains research papers on optical investigations, spectroscopic methods of various kinds, TEM studies including electron diffraction, and, of course, powder X-ray diffraction. However, to the author's knowledge, no paper has been published dealing with detailed crystal structure information on changes resulting due to shock wave compression and release in quartz except recent paper by Fiske et al. [7] who used $^{29}$Si MAS NMR spectroscopy to study Si-O-Si inter-tetrahedral angles within experimentally shocked quartz single crystalline material.

**Samples:** Clear quartz from Švedlár (Slovak Republic) was used as standard. Sandstone from the Coconino Formation, Meteor Crater, Arizona, USA provided naturally impact-shocked sample. The pressure to which this material was subjected can be estimated from the fact that coesite and stishovite are observed in its powder pattern after 24-hour leaching in diluted hydrofluoric acid. Such a sample corresponds to the shock regimes D or E of the pressure calibration for porous sandstone [8,9]. The regime D is characterized by pressures ranging from 5.5 GPa to 13 GPa and post-shock heat from ca 350 °C to 950 °C. In regime E, the pressure ranges from 13 GPa to 30 GPa and post-shock temperature from ca 950 °C to over 1000 °C. The three experimentally shocked had been shock loaded at NASA Johnson Space Center, Houston, Texas, to 21.7 GPa, 26.2 GPa, and 29.8 GPa at 25 °C, respectively.

**Data and their processing:** Powder data were step-scanned in the range 18-150 °2θ CuK$_\alpha$ with 0.015 °2θ CuK$_\alpha$ steps and 15 to 18 sec. count-time per step. They were reduced by programs FULLPROF [10,11], BONDSTR [12], and VOLCAL [13].

**Static compression:** The crystal structure of α-quartz accommodates changes due to elevated static pressures by three various mechanisms based on single-crystal structure studies of Jorgensen [14]. These are: (a) a cooperative rigid rotation of linked [SiO$_4$] tetrahedra; (b) a distortion of [SiO$_4$] tetrahedra caused by changes in bond angles with constant bond lengths; and (c) a decrease in bond lengths. The first mechanism is the most important because it allows to compensate for the largest volume change compared to the other two mechanisms. Rotation of linked tetrahedra with increasing static compression results in the decrease of (Si-O-Si) bond angles (i.e. angles at bridging oxygen) and lengths of tetrahedral edges d(O-O) [2]. Similarly, the distance d(Si-O) within [SiO$_4$] tetrahedra decreases slightly as static pressure increases [15].

**Dynamic compression:** Rietveld crystal structure refinements revealed that unit-cell dimensions increase with increasing shock pressure; at 29.8 GPa the difference in the unit-cell volume amounts 1.6% compared to the unshocked standard. Intra-tetrahedral parameters change with pressure accompanied by a decrease of the tetrahedral volume from about 2.25 Å$^3$ for the unshocked quartz standard to below 1.95 Å$^3$ for the sample shocked at 29.8 GPa. The increase in inter-tetrahedral angles and of distances not only compensates for the decrease of intra-tetrahedral parameters but the increase is large enough to result in the observed increase in unit-cell parameters. The study also reveals that within the material shocked to 29.8 GPa the overall change results in a regularization of the trigonal α-quartz structure and the material approaches the hexagonal symmetry typical of β-quartz despite of strong deformation of individual crystal structure building blocks. The results yielded indicate that dynamic compression is absolutely different process compared to static compression resulting in distinct deformation mechanism.

[1] R.A.F. Grieve, F. Langenhorst, and D. Stöffler, Meteoritics and Planet.Sci., **31** (1996), 6-35.

[2] R.J. Hemley, C.T. Prewitt, and K.J. Kingma, High pressure behavior of silica. In Heaney, P. J., Prewitt, C. T., and Gibbs, G. V., eds., Silica. Reviews in Mineralogy, **29** (1994), 41-81.

[3] F. Langenhorst, Earth and Planet.Sci.Lett., **128** (1994), 683-698.

[4] D. Stöffler, Fortschr.Mineral., **49** (1972), 50-113.

[5] D. Stöffler, Fortschr.Mineral., **51** (1974), 256-289.

[6] D. Stöffler and F. Langenhorst, Meteoritics, **29** (1994), 151-181.

[7] P.S. Fiske, W.J. Nellis, Zhi Xu, and J.F. Stebbins, Amer. Mineral., **83** (1998), 1285-1292.

[8] S.W. Kieffer, P.P. Phakey, and J.M. Christie, Contrib.Mineral.Petrol., **59** (1976), 41-93.

[9] D. Stöffler, J. Non-Crystalline Solids, **67** (1984), 465-502.

[10] J. Rodriguez-Carvajal, Physica B, **192** (1993) 55-69.

[11]; 12] J. Rodriguez-Carvajal, BONDSTR – a computer program, (1995).

[13] L.W. Finger, VOLCAL – a computer program, (1996).

[14] J. D. Jorgensen, J.Appl.Phys., **49** (1978), 5473-5478.

[15] J. Glinnemann, H. E. King Jr., H. Schulz, Th. Hahn, S. J. La Placa, and F. Dacol, Z. Kristall., **198** (1992), 177-212.

# CRYSTAL STRUCTURE OF THE MINERAL KETTNERITE CABI[OF|CO$_3$]

## Jiří Hybler[1], Ivana Císařová[2]

[1]*Institute of Physics, Academy of Sciences of the Czech Republic, Na Slovance 2, 182 21 Praha 8, Czech Republic, E-mail: hybler@fzu.cz*

[2]*Department of Inorganic Chemistry, Faculty of Sciences, Charles University, Hlavova 2030, 128 43 Praha 2, Czech Republic.*

The structure of kettnerite, CaBi[OF|CO$_3$], was refined in the tetragonal cell $a$ 3.787(3) , $c$ 13.508(4) Å, $P4/nmm$, $Z = 2$, $R = 2.30$ % for 217 reflections. (Hybler & Císařová 1999).

The mineral from Krupka, Krušné hory (Ore Mountains), NW Bohemia was described by žák & Syneček (1956, 1957), the association and minerogenetic studies of the deposit were given by žák & Syneček (1957) and žák (1959). The structure was first, but not completely solved by Syneček & žák (1960). They located all atoms except CO$_3$ groups.

The structure contains sheets parallel with (001) consisting of planes of O atoms in a square array at $z = 0$ and planes of Bi atoms slightly below or above the centers of squares (Bi-O-Bi sheets). A similar sheet consists of a plane of F atoms at $z = \frac{1}{2}$ and two planes of Ca atoms (Ca-F-Ca sheets). The triangular CO$_3$ groups are located between these sheets. They are in a positional (or orientational) disorder. The central C atom at ¾, ¾, 0.2511 and one O atom (O2) pointing to the Bi-O-Bi sheet are common for both orientations. The remaining pair of O3 atoms appears in two alternative orientations, perpendicular to each other so that the whole triangle is oriented with equal probability parallel with (100) and (010) planes. The refinement revealed a small peak close to the central C atom which was interpreted after many trials as an extra Bi-atom (or perhaps a part of an extra plane of atoms) replacing with probability 0.038(2) the CO$_3$ group. (Fig.1.)

Similar structures of the minerals bismutite Bi$_2$O$_2$CO$_3$ and beyerite CaBi$_2$O$_2$(CO$_3$)$_2$ were determined by Lagercrantz & Sillén (1948) in tetragonal cells, space group $P4/nmm$. The lattice parameters are $a = 3.87$, $c = 13.69$ Å for bismutite, $a = 3.77$, $c = 21.69$ Å for beyerite. Both structures are formed from Bi-O-Bi sheets, alternating in the later one with planes of isolated Ca atoms. The location and arrangement of the CO$_3$ groups filling the space between Bi-O-Bi sheets of the former or between the Bi-O-Bi sheets and the planes of the Ca atoms of the later structure also remained undetedmined.

Programs used: JANA98 (Petříček & Dušek 1998), PICTUR (Dušek 1993).

1. Dušek, M.: *PICTUR. A molecular graphics program*. Institute of Physics, Academy of Sciences of the Czech Republic, Prague 1993.

2. Hybler, J. & Císařová, I., Submitted to *Eur. J. Mineral*. (1999).

3. Lagercrantz, A. & Sillén, L. G., *Ark. f. Kemi Min. o. Geol.*, **25A** (1948), 1-21.

4. Petříček, V. & Dušek, M.: *JANA98, Crystallographic computer program for standart, modulated and composite structures.* Institute of Physics, Academy of Sciences of the Czech Republic, Prague 1998. (unpublished, but available at http://www-xray.fzu.cz/jana/jana98.html).

5. Syneček, V. & žák, L., *Czech. J. Phys.*, **B10** (1960), 195-207.

6. žák, L., *Chemie der Erde*, **20** (1959), 81-103.

7. žák, L. & Syneček, V., *Čas. Min. a Geol.*, **1** (1956), 195-197 (in Czech).

8. žák, L. & Syneček, V., *Acta Univ. Carol. Geol.*, **3** (1957), 1-46 (in Czech).

# METHOD FOR INVESTIGATION OF BECOMING OF MCM-41 MESOPORIC ZEOLITES FROM SOLUTIONS ON CONVENTIONAL DIFFRACTOMETER

## J. Had

*Institute of Chemical Technology, Technická 5, 166 28 Prague 6, Czech Republic.*

Recently a new procedure for the synthesis of siliceous mesoporous material MCM-41 with regular morphology using a surfactant as a structure directing agent was developed. [1] This synthesis route is based on the precipitation from an isotropic reaction mixture at ambient temperature. The decrease in pH, which causes the formation of solid particles, is achieved by the hydrolysis of ethyl acetate (EtAc). Real-time *in situ* study of the formation of the ordered phase was performed.[2]

MCM-41 zeolite is a material with a high degree of pore ordering and hexagonal symmetry. Four reflections are discernible in the range of $2° < 2\Theta < 9°$ (CoK$\alpha$), which can be indexed as (100), (110), (200) and (210). The MCM-41 molecular sieve was synthesized from the reaction mixture, which was prepared directly in polypropylene bottle. 9.8 g of cetyltrimethylammonium bromide (CTABr) followed by 10 g of solid $Na_2SiO_3$ were dissolved in 650 ml of distilled water, resulting in a clear solution. Afterwards 15 ml of EtAc were quickly added under vigorous stirring. After 30 sec the stirring was stopped. 3 ml sample was taken from the reaction mixture just when the stirring after the addition of EtAc was stopped and was transferred into the XRD cuvette.

The *in situ* XRD measurements were performed on (100) diffraction line in the range of $2\Theta$ from 1.8 to 3.0 degrees. Commercial PMM sample holder of Seifert C o. was used. It is square shape 30x30 mm holder with 26x26x1 mm cutting. There was a little corrugation made into the upper edge. The holder was bespred with polyethylene foil „Mikroten" of 10 micrometers thickness. Absorption of such foil was found negligible. Then the foil was stretched and glued with the adhesive tape to the back side of the holder properly enough to be waterproof. Sample was injected with the syringe through corrugation in the holder to fill up the cutting totally. The sample was measured in vertical position. Such position has advantage in elimination of particle sedimentation as far as irradiated area is 10 mm wide bar in the middle of the holder. According to the Stokes law, particle concentration in irradiated volume is under experimental conditions constant due to the small particle size in the beginning of the reaction , high viscosity in the later stages and small difference in density of the particles and of the liquid phase.

Experimental conditions of x-ray measurement: System XRD 3000 P fy. Seifert, BDR. Tube output 35 kV /35mA, divergence slit 0,25° ,scintillation counter with 0,2mm receiving slit, secondary graphite monochromator. Step mode, 0,03° (2theta)/step, 1sec/step. Such short time was chosen to perceive kinetic of the phase formation. Immediately after the end of one measurement the next measurement of the same interval followed.

Two different synthesis were investigated. The temporal dependencies of the integral net intensity $I_{net}$ of (100) reflections and the interplanar spacing $d_{100}$ for MCM-41 and BMS (bimodal silica) were compared. From both dependencies of $I_{net}$ it follows that the reaction mixture immediately after the addition of EtAc is an isotropic solution without any ordering detectable by XRD. With BMS the initially rapid changes of $I_{net}$ and $d_{100}$ approach limiting values after ca 60 min. With MCM-41 this tendency is less evident, *i.e.* the process of formation and growth of solid particles is slower.

1. Rathousky J., Zukalová M., Zukal A., Had J.: *Collect. Czech. Commun.*, Vol . **63** (1998), p.1893-1906.

2. Rathousky J., Schulz-Ekloff G., Had J., Zukal A.: *Physical Chemistry – Chemical Physic*, in print.

---

# SYNTHETIC SCHREIBERSITES (Fe,Ni)₃P: IRON AND NICKEL DISTRIBUTION IN NON-EQUIVALENT SITES OF THEIR CRYSTAL STRUCTURE

## R. Skála and M. Drábek,

*Czech Geological Survey, Klárov 3/131, CZ-11821 Praha 1, Czech Republic, e-mail addresses: skala@cgu.cz, drabek@cgu.cz*

**Experimental details:** Phosphides were synthesized in evacuated, sealed silica tubes in which weighed amounts of the starting elements were heated for several days in horizontal tube furnaces at 900 °C. Temperature was measured with Pt-PtRh thermocouples and is accurate to ± 3 °C. Runs were repeatedly re-ground under acetone and re-heated at given temperature. Experimental charges were quenched by dropping them in ice water. Phosphides were synthesized from mixes of iron (JMC - iron sponge, 99.999% purity), nickel (SPEX - nickel powder 99.999% purity) and red amorphous phosphorus (FLUKA, purum). Iron and nickel were heated for 4 hours in a stream of hydrogen. Phosphorus was washed in distilled water and acetone, and then dried under vacuum. The reaction products were examined by reflected light microscopy and electron probe microanalysis. Some runs are accompanied by very small quantities of iron phosphates.

Two phosphide compositions – $Fe_3P:Ni_3P = 3:1$ and $Fe_3P:Ni_3P = 1:3$ resulting in empirical formulae $Fe_{2.25}Ni_{0.75}P$ and $Ni_{2.25}Fe_{0.75}P$, respectively, were selected for powder diffraction study. Powder diffraction data for Rietveld crystal structure refinements were collected using a Philips X'Pert MPD diffractometer equipped with Cu ceramic tube operated at 40 kV voltage and 40 mA tube current. Background due to fluorescence in the sample was lowered by use of secondary monochromator. Step-scanned data were acquired in the range 10-150° $2\Theta$ with step width 0.02° $2\Theta$ and exposure per a step 8 sec. Refinements of crystal structure were carried out by program FullProf.98 [1,2]. Refined parameters were fractional coordinates, unit-cell dimensions, half-width parameters, and preferred orientation parameter. Isotropic temperature factors remained fixed during refinements. To eliminate limi-

*Results of Rietveld crystal structure refinement for the models with the best fit. Final atomic coordinates, site occupancies, unit-cell parameters, and R-factors. Isotropic temperature factors $B_{iso}$ were fixed to 0.4 $\text{Å}^2$ during the refinement for all sites.*

| Site | Atom | Overall composition: $Fe_{2.25}Ni_{0.75}P$ | | | | Overall composition: $Ni_{2.25}Fe_{0.75}P$ | | | |
|------|------|-----------|-----------|----------|--------|-----------|-----------|----------|--------|
| | | x | y | z | S.O.F. | x | y | z | S.O.F. |
| Me1 | Ni | 0.04842(7) | 0.112797) | 0.250(3) | 1.000 | 0.0808(7) | 0.1078(7) | 0.243(2) | 0.75 |
| | Fe | | | | 0.000 | | | | 0.25 |
| Me2 | Ni | 0.3571(7) | 0.0293(9) | 0.991(2) | 0.833 | 0.3573(7) | 0.0335(8) | 0.965(2) | 0.00 |
| | Fe | | | | 0.167 | | | | 1.00 |
| Me3 | Ni | 0.1682(8) | 0.2199(7) | 0.738(3) | 0.417 | 0.1681(7) | 0.21219(6) | 0.726(2) | 0.00 |
| | Fe | | | | 0.583 | | | | 1.00 |
| X | P | 0.3002(12) | 0.0457(14) | 0.472(3) | 1.000 | 0.2910(10) | 0.0465(12) | 0.469(2) | 1.00 |
| | a[Å] | 9.0633(2) | $R_p$[%] | 9.35 | | a[Å] | 8.9973(3) | $R_p$[%] | 6.71 |
| | c[Å] | 4.4638(2) | $R_{wp}$[%] | 12.2 | | c[Å] | 4.4291(2) | $R_{wp}$[% | 9.45 |
| | V[$\text{Å}^3$] | 366.67(2) | $\chi^2$ | 1.02 | | V[$\text{Å}^3$] | 358.54(2) | $\chi^2$ | 1.07 |

tations of the Rietveld method due chiefly to close scattering factors for nickel and iron, we modeled several possible Fe/Ni site occupancies and fix site occupation factors (SOF) accordingly. Then we refined these constrained models. The quality of the fit was finally tested according to a value of Bragg R-factor $R_B$.

**Discussion:** Results for models with the best fit are listed in table below. Fe/Ni-distribution over non-equivalent crystal structure sites for phase of $Fe_{2.25}Ni_{0.75}P$ composition is close to a general trend met in structure refinements of natural schreibersites using both single-crystal methods [3,4] and Rietveld method from powder data [5]. Results for $Ni_{2.25}Fe_{0.75}P$ phase indicates similar trend – site Me1 is preferentially occupied by iron. Based on these observations we can postulate a general trend on the site occupancies in schreibersites – the site Me1 usually contain most of iron available, other two sites are occupied

by rest of iron with dominant Fe content in Me2. This trend, however, may be disturbed by the conditions of schreibersite formation ruling out diffusion and partitioning coefficients, constituting thus the method presented as potential procedure for estimating of cooling rates for differentiated iron meteorites.

[1] J. Rodriguez-Carvajal *Physica B*, **192**, (1993)55-69.

[2] J. Rodriguez-Carvajal FullProf 98 – a computer program, (1998).

[3] F. D. Doenitz *Zeit. Kristall*., **144**, (1971) 534–535.

[4] R. Skála and I. Císařová *LPSC*, **XXX**, (1999).

[5] R Skála and J. Frýda LPSC, ***XXVII***, (1995) 1211–1212.